Engineering Notes

Distributed Cooperative Guidance for Multivehicle Simultaneous Arrival Without Numerical Singularities

Kang Li*
Westlake University, 310024 Hangzhou, People's Republic of China
Jianan Wang†
Beijing Institute of Technology, 100081 Beijing, People's Republic of China
Chang-Hun Lee‡
Korea Advanced Institute of Science and Technology, Daejeon 34141, Republic of Korea
Rui Zhou§
Beijing University of Aeronautics and Astronautics, 10083 Beijing, People's Republic of China
and
Shiyu Zhao¶
Westlake University, Westlake Institute for Advanced Study, 310024 Hangzhou, People's Republic of China

https://doi.org/10.2514/1.G005010

I. Introduction

COOPERATIVE guidance of multiple vehicles for simultaneous arrival is an effective way to increase the success rate of, for example, missile–target interception. The seminal research work in Ref. [1] proposed an impact time control guidance (ITCG) law and applied ITCG to multimissile simultaneous arrival tasks. This work has inspired extensive consequent research work on cooperative guidance. The existing cooperative guidance approaches could be classified into two streams. In the first stream, guidance laws are designed for single vehicles [2–5] and then applied to cooperative guidance of multiple vehicles by prescribing the same desired arrival time for each vehicle in advance [1] or letting multiple vehicles synchronize their arrival time automatically during engagement [6]. In the second stream, the interaction among multiple vehicles is considered in the design of cooperative guidance laws from the very beginning [7,8].

Although many cooperative guidance laws have been proposed up to now, these guidance laws still face many challenges. First, many guidance laws suffer from numerical singularities, due to which the guidance commands would diverge to infinity when the vehicle–target range or velocity heading angle is close to zero [1,9]. Second, most of the existing guidance laws rely on accurate estimation of time to go [1,4], which is difficult to estimate accurately and has motivated many studies aiming to increase the estimation accuracy of time to go [10,11]. Third, another important challenge is to incorporate network interaction among multiple vehicles in guidance law design. Cooperative guidance is a networked dynamical system, which suffers from many practical problems such as limited communication range, communication delay, and switching topologies. These important problems, however, are rarely analyzed in the literature of cooperative guidance due to the highly nonlinear system dynamics.

One promising tool to handle network interaction is consensus algorithms that can synchronize certain states over a network in distributed manners. Consensus algorithms have been well studied in the literature [12–15] and have been proven to be effective in the presence of many challenging issues such as communication delay and switching topologies [16]. In fact, consensus algorithms have already been adopted in some existing cooperative guidance approaches, which exhibit promising guidance performance [9,17–19]. However, these guidance laws have some problems. For example, the guidance strategies proposed in Refs. [9,17] are two-stage, and hence the cooperative guidance laws must be switched to pure proportional navigation guidance (PNG) at the final stage of guidance. The consensus-based guidance law proposed in Ref. [18] does not require multistage implementation. However, the guidance law is based on online optimization, and hence does not have an analytical expression. The work in Ref. [19] specifically analyzes network structures for cooperative guidance under unreliable and noisy communication. However, this work adopts the two-layer guidance structure [6], where the bottom layer is based on ITCG and the top layer is based on consensus algorithms. Note that ITCG also suffers from numerical singularities when the vehicle–target range is zero.

To overcome the drawbacks of the existing guidance laws, we first propose a new vehicle–target engagement model and convert it to a double-integrator model by feedback linearization. This double-integrator model lays a theoretical foundation for designing and analyzing arrival time coordination control. We then propose a novel distributed cooperative guidance law based on this model. The proposed guidance law overcomes many drawbacks of the guidance laws in the literature and possesses the following attractive features.

1) The proposed guidance law has a concise analytical expression, which is a summation of a PNG term for target pursuing and a coordination control term for arrival time synchronization. When arrival time is synchronized, the proposed guidance law degenerates to pure PNG. This type of structure, which is also called biased PNG [20,21], is favorable in guidance law design because PNG is the most widely used guidance law [22].

2) The proposed guidance law is free of any numerical singularities at which the acceleration command would be infinite. This is opposed to Refs. [1,9], where numerical singularities require the guidance laws to be switched to PNG in the final stage.

3) The proposed guidance law does not require the estimation of time to go as opposed to many existing cooperative guidance laws [1,4,10,11]. That is because the guidance law is designed to synchronize the normalized range to go and closing speed.

4) The proposed guidance law is distributed because each vehicle is merely required to know a small amount of information of their nearest neighboring vehicles. This is different from the guidance laws

Received 9 December 2019; revision received 2 March 2020; accepted for publication 11 March 2020; published online 23 April 2020.

*Ph.D. Candidate, School of Engineering; likang32@westlake.edu.cn.
†Associate Professor, School of Aerospace Engineering; wangjianan@ieee.org.
‡Assistant Professor, Department of Aerospace Engineering; lckdgns@kaist.ac.kr.
§Professor, School of Automation Science and Electrical Engineering; zhr@buaa.edu.cn.
¶Assistant Professor, School of Engineering; zhaoshiyu@westlake.edu.cn (Corresponding Author).

that require each vehicle to be able to communicate with all the other vehicles [7].

5) The parameters in the proposed guidance law could be selected in a straightforward way to ensure effective guidance performance in a wide range of engagement scenarios. This is different from some existing guidance laws such as Ref. [7], where the parameter in the guidance law must be calculated in advance based on the initial states of all vehicles.

Both two-dimensional (2-D) and three-dimensional (3-D) versions of the guidance law are proposed. Comprehensive simulation shows that the guidance laws could work effectively in a wide range of guidance scenarios, even in the presence of acceleration saturation, communication delay, and measurement noises. It is also demonstrated that the proposed guidance law still performs robustly in some extreme scenarios, where the initial time-to-go difference among multiple vehicles is large or the initial velocity leading angle of each vehicle is large.

II. Problem Statement

Consider $n \geq 2$ mobile vehicles and one stationary target in the plane. The position coordinate of the target expressed in an inertial frame is denoted as (x_T, y_T) and the position of vehicle i is (x_i, y_i), where $i = 1, \ldots, n$. The speed and heading angle of vehicle i are denoted as v_i and θ_i, respectively. Here, $v_i > 0$ is constant and θ_i is defined as positive counterclockwise and negative clockwise (see Fig. 1). The motion of vehicle i is governed by

$$\dot{x}_i = v_i \cos\theta_i, \qquad \dot{y}_i = v_i \sin\theta_i, \qquad \dot{\theta}_i = a_i / v_i$$

where a_i is the lateral acceleration command to be designed. By the definition of θ_i, a_i is positive (negative, respectively) when the acceleration points to the left-hand (right-hand, respectively) side of the velocity vector.

Let $r_i \geq 0$ be the range from vehicle i to the target, λ_i the line-of-sight (LOS) angle, and η_i the velocity leading angle (see Fig. 1). We define η_i and λ_i to be positive counterclockwise and negative clockwise. As a result, $\theta_i = \eta_i + \lambda_i$. Moreover, it follows from their definitions that $\dot{r}_i = -v_i \cos\eta_i$ and $\dot{\lambda}_i = -v_i \sin\eta_i / r_i$.

The interaction among the vehicles is described by a graph $\mathcal{G} = (\mathcal{V}, \mathcal{E})$, which consists of a vertex set $\mathcal{V} = \{1, \ldots, n\}$ and an edge set $\mathcal{E} \subseteq \mathcal{V} \times \mathcal{V}$. The directed edge $(i, j) \in \mathcal{E}$, pointing from vertex i to vertex j, indicates that information flows from vehicle i to vehicle j, and hence i is a neighbor of j. The set of neighbors of vertex i is denoted as $\mathcal{N}_i = \{k \in \mathcal{V} : (k, i) \in \mathcal{E}\}$.

The problem to be solved in this Note is how to design $\{a_i\}_{i=1}^n$ to guide all the vehicles to arrive at the target simultaneously given random initial conditions.

III. Proposed Cooperative Guidance Law

This section first presents a new vehicle–target engagement model and then proposes a cooperative guidance law based on this model.

A. New Engagement Model

Consider the body frame of vehicle i. The origin of the body frame is located at the center of gravity, and the x axis is aligned with the velocity heading (see Fig. 2). The coordinate of the target in the body frame is $(x_{T,B}, y_{T,B})$. Although the target is stationary in the inertial reference frame, its coordinate in the body frame is time varying.

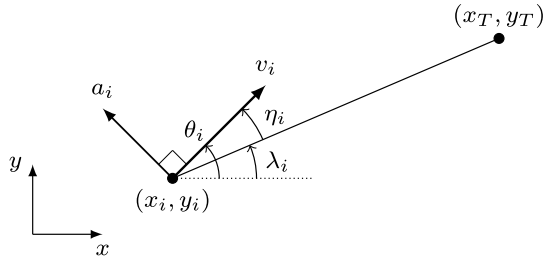

Fig. 1 2-D vehicle–target engagement geometry.

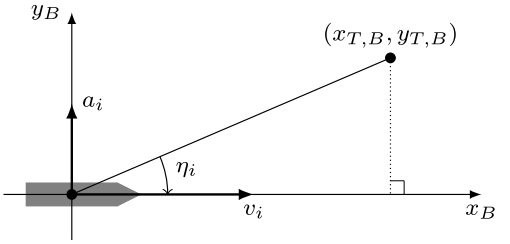

Fig. 2 2-D vehicle–target engagement geometry in the body frame. Note that η_i is defined to be positive counterclockwise, and hence the value of η_i shown in the figure is negative.

Note that $-r_i \sin\eta_i = y_{T,B}$. Taking the time derivative on both sides of this equation gives

$$\dot{r}_i \sin\eta_i + r_i \cos\eta_i \dot{\eta}_i = -\dot{y}_{T,B} \tag{1}$$

In practice, η_i is usually small because the terminal homing guidance phase generally follows a precise guidance handover from a proper midcourse guidance law. When η_i is small, it holds that $\sin\eta_i \approx \eta_i$ and $\cos\eta_i \approx 1$; then Eq. (1) becomes

$$\dot{r}_i \eta_i + r_i \dot{\eta}_i = -\dot{y}_{T,B}$$

Taking the time derivative on both sides of the preceding equation yields

$$\ddot{r}_i \eta_i + 2\dot{r}_i \dot{\eta}_i + r_i \ddot{\eta}_i = -\ddot{y}_{T,B} = a_i \tag{2}$$

Inspired by feedback linearization, we design

$$a_i = \eta_i u_i + 2\dot{r}_i \dot{\eta}_i + r_i \ddot{\eta}_i \tag{3}$$

where u_i is a new input command to be designed. Substituting Eq. (3) into Eq. (2) gives

$$\ddot{r}_i = u_i \tag{4}$$

As a result, the nonlinear engagement model is converted to a linear double-integrator model, which can be used to design arrival time coordination control, as will be shown in the next subsection. Furthermore, it follows from $\eta_i = \theta_i - \lambda_i$ that $\dot{\eta}_i = \dot{\theta}_i - \dot{\lambda}_i = a_i / v_i - \dot{\lambda}_i$; then, Eq. (3) becomes $a_i = \eta_i u_i + 2\dot{r}_i (a_i / v_i - \dot{\lambda}_i) + r_i \ddot{\eta}_i$. Because $\dot{r}_i = -v_i \cos\eta_i \approx -v_i$, we further have $3a_i = \eta_i u_i + 2v_i \dot{\lambda}_i + r_i \ddot{\eta}_i$, which could be rewritten as

$$a_i = \eta_i u_i + \frac{2}{3} v_i \dot{\lambda}_i + \frac{1}{3} r_i \ddot{\eta}_i \tag{5}$$

where the coefficient $1/3$ in the first term is merged into u_i without loss of generality.

B. Coordination Control of Arrival Time

Based on Eq. (4), we next design u_i to synchronize the arrival time of the vehicles. In particular, our aim is to design u_i such that

$$\left| \frac{r_i}{\dot{r}_i} - \frac{r_j}{\dot{r}_j} \right| \to 0 \tag{6}$$

for all i and j. Here, $r_i / \dot{r}_i$ could be interpreted as an estimate of the time to go of vehicle i. Because different vehicles may have different constant speed values, we define the normalized range and normalized closing speed, respectively, as

$$\bar{r}_i = \frac{r_i}{v_i}, \qquad \dot{\bar{r}}_i = \frac{\dot{r}_i}{v_i}$$

Because Eq. (6) is ensured if $|\bar{r}_i - \bar{r}_j| \to 0$ and $|\dot{\bar{r}}_i - \dot{\bar{r}}_j| \to 0$, we design u_i to synchronize $\{\bar{r}_i\}$ and $\{\dot{\bar{r}}_i\}$:

$$u_i = v_i \sum_{j \in \mathcal{N}_i} w_{ij}[c_1(\bar{r}_j - \bar{r}_i) + c_2(\dot{\bar{r}}_j - \dot{\bar{r}}_i)] \tag{7}$$

where w_{ij}, c_1, and c_2 are constant positive coefficients. In particular, w_{ij} is the weight for edge (j, i), and c_1 and c_2 represent the contribution ratio between the normalized range and normalized closing speed. Substituting Eq. (7) into $\ddot{\bar{r}}_i = u_i/v_i$ yields

$$\ddot{\bar{r}}_i = \sum_{j \in \mathcal{N}_i} w_{ij}[c_1(\bar{r}_j - \bar{r}_i) + c_2(\dot{\bar{r}}_j - \dot{\bar{r}}_i)] \tag{8}$$

Equation (8) is a second-order consensus protocol that has been well studied in the literature [16,23]. When the underlying graph is fixed and undirected, consensus is achieved if, and only if, the graph is connected ([16] corollary 4.3). When the underlying graph is directed, consensus is archived if, and only if, the underlying graph contains a spanning tree and the coefficients satisfy certain conditions ([23] theorem 1).

Because the second-order consensus system [Eq. (8)] has been well studied in the literature, we do not need to repeat the analysis here. It is worth mentioning that the protocol [Eq. (8)] exhibits good performance in the presence of many challenging practical issues such as communication delay [23,24] and switching network topologies [25]. This is an important reason why the cooperative guidance law proposed later exhibits robust performance.

Finally, note that Eq. (7) allows vehicles to have different constant speed values. The key reason is that u_i is designed to synchronize the normalized range and closing speed values $\{\bar{r}_i\}_{i=1}^n, \{\dot{\bar{r}}_i\}_{i=1}^n$ instead of the absolute ones $\{r_i\}_{i=1}^n, \{\dot{r}_i\}_{i=1}^n$. In fact, this is required by the nature of the guidance problem. Hypothetically, suppose that u_i is designed to achieve $|r_i - r_j| \to 0$ and $|\dot{r}_i - \dot{r}_j| \to 0$. Even though $r_i/\dot{r}_i$ could converge to the same value, if vehicles have different constant speed values, it is impossible to ensure $\eta_i, \eta_j \to 0$. That is because $|\dot{r}_i - \dot{r}_j| \to 0$ implies $|-v_i \cos\eta_i + v_j \cos\eta_j| \to 0$. If $v_i \neq v_j$, it is impossible to have $\eta_i, \eta_j \to 0$. In this sense, Eq. (7) is a generalized version of the coordination control law in Ref. [9], where all the vehicles are assumed to have the same constant speed.

C. Proposed Cooperative Guidance Law

Substituting u_i in Eq. (7) into a_i in Eq. (5) gives a cooperative guidance law. One merit of this guidance law is that it is free of numerical singularities. Moreover, this guidance law has a clear structure: The first term is a coordination control command for time synchronization. The second term is a PNG command with the navigation constant as $2/3$. The third term contains the second-order derivative $\ddot{\eta}_i = \dot{a}_i/v_i - \ddot{\lambda}_i$, which is difficult to obtain accurately in practice, or even in numerical simulation. As we will show in the following, the third term is not dominant and a modified guidance law without this term still has effective and stable performance.

To inherit its numerical-singularity-free property and avoid its unfavorable properties, we modify Eq. (5) to propose a new distributed cooperative guidance (DCG) law:

$$\begin{aligned} a_i &= Nv_i\dot{\lambda}_i + \eta_i u_i \\ &= Nv_i\dot{\lambda}_i + \eta_i v_i \sum_{j \in \mathcal{N}_i} w_{ij}\left[c_1\left(\frac{r_j}{v_j} - \frac{r_i}{v_i}\right) + c_2\left(\frac{\dot{r}_j}{v_j} - \frac{\dot{r}_i}{v_i}\right)\right] \end{aligned} \tag{9}$$

where $N = 3$; and w_{ij}, c_1, and c_2 are constant positive parameters. The proposed DCG in Eq. (9) consists of two terms. The first term is the classic PNG command for the purpose of target pursuing. The second term is a coordination control command for the purpose of arrival time synchronization. Unlike Eq. (5), the navigation constant in the first term is modified to $N = 3$. That is because, when the arrival time is synchronized, the second term would vanish and the guidance law becomes pure PNG, which must have an appropriate navigation constant. The value of $N = 3$ leads to stable PNG performance and is widely used in the literature [1,7]. DCG in Eq. (9) also omits the third term $r_i\ddot{\eta}_i$ in Eq. (5). That is because, first, $\ddot{\eta}_i$ is difficult to obtain accurately in either practice or numerical simulation and, second, omitting this term does not yield any performance decay, as we will show by simulation later.

DCG has some merits as follows. It has a biased-PNG structure, which is favorable in guidance law design because PNG is the most widely used guidance law. DCG is free of numerical singularities that would cause infinite acceleration commands. As a result, it is not required to switch to another guidance law during engagement. Moreover, this guidance law is distributed because the guidance command of a vehicle merely relies on a small amount of information of its neighbors. The measurements required by the guidance law are independent of any coordinate frame and easy to obtain in practice.

Some important properties of DCG are discussed in the following:

1) If we consider the second-order consensus protocol [Eq. (8)] independently, the converged value of $\dot{\bar{r}}_i(t)$ equals a weighted average of their initial values ([23] theorem 1). However, in the guidance problem since $\dot{\bar{r}}_i = \dot{r}_i/v_i = -v_i\cos\eta_i/v_i = -\cos\eta_i$, $\dot{\bar{r}}_i \to -1$ if, and only if, $\eta_i \to 0$. Although η_i would converge to zero in the guidance problem, $\dot{\bar{r}}_i$ would converge to -1.

2) In the second term of Eq. (9), the sign of η_i plays a critical role for vehicle i adjusting its trajectory correctly to control its arrival time. To see that, recall that $a_i = Nv_i\dot{\lambda}_i + \eta_i u_i$. If $u_i = \ddot{r}_i > 0$, then vehicle i aims to increase r_i to increase its arrival time. In this case, if v_i is on the left-hand side of the LOS, for example, then $\eta_i > 0$; hence, the synchronization term $\eta_i u_i > 0$ will turn the velocity heading further to the left to take a detour, which is the desired behavior for arrival time control.

3) When $\eta_i = 0$, the second term would vanish and vehicle i would cut off its interaction with its neighbors. However, $\eta_i = 0$ means that vehicle i's velocity points directly to the target, which ensures successful target interception. In fact, this problem also exists in the classic cooperative guidance law proposed in Ref. [7]. The recent work of Ref. [26] modified the guidance law in Ref. [7] to solve this problem. Similar techniques could be applied to modify our proposed guidance law. However, we would like to mention that such a "problem" may be a merit rather than a drawback. That is because the guidance law naturally places target pursuing as the highest priority and time synchronization as secondary. After all, successful target interception is the most important task for guidance.

Remark 1: For the purpose of comparison, it is meaningful to revisit the engagement model and guidance law proposed in Ref. [9]. In particular, it follows from $\dot{r}_i = -v_i\cos\eta_i$ that

$$\ddot{r}_i = v_i\sin\eta_i\dot{\eta}_i = v_i\sin\eta_i(\dot{\theta}_i - \dot{\lambda}_i) = v_i\sin\eta_i\left(\frac{a_i}{v_i} + \frac{v_i\sin\eta_i}{r_i}\right) \tag{10}$$

By feedback linearization, Ref. [9] designed

$$a_i = \frac{u_i}{\sin\eta_i} - \frac{v_i^2\sin\eta_i}{r_i} \tag{11}$$

where u_i is a new input. Substituting Eq. (11) into Eq. (10) gives $\ddot{r}_i = u_i$, which is a double-integrator model. Based on this model, Ref. [9] designed a consensus-based coordination control law to achieve simultaneous arrival. However, the acceleration command in Eq. (11) has two critical singularities:

$$\sin\eta_i = 0, \qquad r_i = 0$$

Due to the singularities, a_i would diverge to infinity when $\eta_i \to 0$ or $r_i \to 0$. The singularity is not able to be avoided if the rigorous model [Eq. (10)] is used.

D. Parameter Selection

The values of w_{ij}, c_1, and c_2 in Eq. (9) must be selected properly to achieve good guidance performance. For a group of homogenous vehicles, we may simply set w_{ij} to the same value w for all i and j. Because there are only two degrees of freedom in the three parameters w, c_1, and c_2, we suppose $c_1 + c_2 = 1$ without loss of generality. Then, we only need to focus on the selection of w and c_2.

The value of w determines the relative weight of the second consensus term with respect to the first PNG term in Eq. (9). In particular, if w is close to zero such that the first PNG term is dominant, then the performance of DCG is similar to PNG. In this case, the target is intercepted before the arrival time has synchronized. If w is sufficiently large, such that the first and second terms are well balanced, then both target interception and arrival time synchronization could be successfully archived. However, if w is too large, such that the second consensus term is dominant, then DCG is close to a consensus protocol, and consequently could not ensure target interception.

The value of c_2 determines the convergence of the second-order consensus system [Eq. (8)]. In particular, Eq. (8) is convergent if, and only if, the underlying graph has a spanning tree and the parameters c_1 and c_2 satisfy ([23] theorem 1)

$$\frac{c_2^2}{c_1} > \kappa \tag{12}$$

where $\kappa \geq 0$ is a lower bound determined by the underlying graph. Substituting $c_1 = 1 - c_2$ into Eq. (12) gives $c_2 > (-\kappa + \sqrt{\kappa^2 + 4\kappa})/2$. If the underlying graph is fixed and undirected, $\kappa = 0$, and hence any positive value of c_2 could ensure the convergence of Eq. (8). If the underlying graph is fixed and directed, then $\kappa > 0$, and its value could be calculated according to theorem 1 of Ref. [23]. In this case, c_2 must be sufficiently large to ensure the convergence of Eq. (8).

On the other hand, c_2 should not be too close to one; otherwise, it may result in the failure of arrival time synchronization. To see that, consider the extreme case of $c_2 = 1$ and $c_1 = 0$; then, the second-order consensus protocol [Eq. (8)] downgrades to

$$\ddot{\bar{r}}_i = \sum_{j\in\mathcal{N}_i} w_{ij}(\dot{\bar{r}}_j - \dot{\bar{r}}_i), \qquad i \in \mathcal{V} \tag{13}$$

which is a first-order consensus protocol of $\dot{\bar{r}}_i$. Then, Eq. (13) only ensures $|\dot{\bar{r}}_i - \dot{\bar{r}}_j| \to 0$, whereas $|\bar{r}_i - \bar{r}_j| \to 0$ is not guaranteed. As a result, the arrival times of different vehicles may not synchronize. Nevertheless, simulation shows that $\dot{\bar{r}}_i$ would converge to -1, and consequently $\eta_i \to 0$ in this case. As a result, when $c_2 = 1$, successful target interception could still be achieved, although the arrival time may not synchronize.

In summary, the preceding analysis provides a guideline to select the values of w and c_2. However, their values still require fine tuning according to specific application scenarios. It is worth noting that guidance convergence is more important than time synchronization. In certain cases, time synchronization must be sacrificed if it may undermine guidance convergence. Some specific suggestions on the value selection of w and c_2 will be given in the simulation section (Sec. V).

IV. Extension to Three-Dimensional Guidance

In the 3-D space, suppose the position, velocity, and acceleration vectors of vehicle i are $\boldsymbol{p}_i, \boldsymbol{v}_i, \boldsymbol{a}_i \in \mathbb{R}^3$, respectively. The motion model of vehicle i is

$$\dot{\boldsymbol{p}}_i = \boldsymbol{v}_i, \qquad \dot{\boldsymbol{v}}_i = \boldsymbol{a}_i \tag{14}$$

Here, $\|\boldsymbol{v}_i\| = v_i$ is constant and $\boldsymbol{a}_i$ is always orthogonal to $\boldsymbol{v}_i$. Note that we do not use the model relying on the azimuth and elevation angles, as in Ref. [27,28]. That is because the azimuth angle is not well defined when the elevation angle equals ± 90 deg, or equivalently when the velocity vector is parallel to the z axis. The model in Eq. (14) is more general because it does not suffer from any singularities.

The proposed 3-D version of DCG is

$$\boldsymbol{a}_i = a_i \boldsymbol{n}_i \tag{15}$$

where

$$a_i = N v_i\left(-\frac{v_i \sin\eta_i}{r_i}\right) + \eta_i v_i \sum_{j\in\mathcal{N}_i} w_{ij}\left[c_1\left(\frac{r_j}{v_j} - \frac{r_i}{v_i}\right) + c_2\left(\frac{\dot{r}_j}{v_j} - \frac{\dot{r}_i}{v_i}\right)\right] \tag{16}$$

and $\boldsymbol{n}_i \in \mathbb{R}^3$ is a unit normal vector that represents the direction of the acceleration:

$$\boldsymbol{n}_i = -\frac{\boldsymbol{P}_{\boldsymbol{v}_i}\boldsymbol{g}_i}{\|\boldsymbol{P}_{\boldsymbol{v}_i}\boldsymbol{g}_i\|} \tag{17}$$

where $\boldsymbol{g}_i \in \mathbb{R}^3$ is the unit vector along the LOS, and

$$\boldsymbol{P}_{\boldsymbol{v}_i} = \boldsymbol{I} - \frac{\boldsymbol{v}_i}{\|\boldsymbol{v}_i\|}\frac{\boldsymbol{v}_i^T}{\|\boldsymbol{v}_i\|} \in \mathbb{R}^{3\times 3}$$

Here, $\boldsymbol{I} \in \mathbb{R}^{3\times 3}$ is the identity matrix and $\boldsymbol{P}_{\boldsymbol{v}_i}$ is an orthogonal projection matrix satisfying $\boldsymbol{P}_{\boldsymbol{v}i}^T = \boldsymbol{P}_{\boldsymbol{v}_i}$ and $\boldsymbol{P}_{\boldsymbol{v}i}^2 = \boldsymbol{P}_{\boldsymbol{v}_i}$. Note that $\boldsymbol{P}_{\boldsymbol{v}_i}\boldsymbol{g}_i$ is the orthogonal projection of $\boldsymbol{g}_i$ onto the orthogonal complement of $\boldsymbol{v}_i$ (see Fig. 3). As a result, $\boldsymbol{n}_i$ is always orthogonal to $\boldsymbol{v}_i$.

Two remarks about Eq. (16) are given in the following. First, the acceleration command in Eq. (16) could be obtained from the 2-D DCG in Eq. (9) by replacing $\dot{\lambda}_i$ with $-v_i \sin\eta_i / r_i$. Note that η_i in Eq. (16) is always a positive value in $[0, \pi]$ in the 3-D case, whereas it could be negative in the 2-D case. Second, note that $\|\boldsymbol{P}_{\boldsymbol{v}_i}\boldsymbol{g}_i\|$ is on the denominator of $\boldsymbol{n}_i$ in Eq. (17). It follows from $\|\boldsymbol{P}_{\boldsymbol{v}_i}\boldsymbol{g}_i\| = \sin\eta_i$ that $\|\boldsymbol{P}_{\boldsymbol{v}_i}\boldsymbol{g}_i\| = 0$ if, and only if, $\eta_i = 0$ or $\eta_i = \pi$.

1) When $\eta_i = 0$, $\sin\eta_i$ on the denominator of $\boldsymbol{n}_i$ is cancelled by $\sin\eta_i$ and η_i in a_i in Eq. (16). As a result, there is no numerical singularity in this case.

2) When $\eta_i = \pi$, the velocity is pointing to the opposite direction of the target. This extreme case rarely occurs in practice. Nevertheless, to handle this extreme case, $\boldsymbol{n}_i$ could be chosen as any vector that is orthogonal to the LOS to steer the vehicle's heading away from this direction.

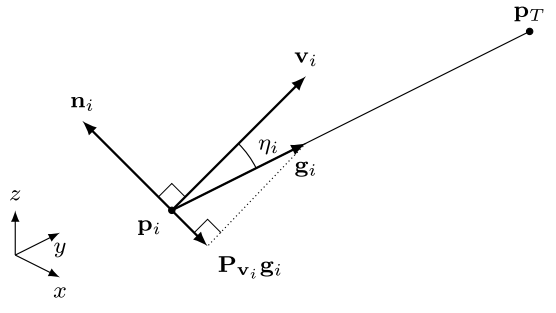

Fig. 3 3-D vehicle–target engagement geometry.

V. Numerical Simulation

The simulation setup is as follows. There are two independent parameters, w and c_2, in the proposed guidance laws in Eq. (9) and (15). Note that $c_1 = 1 - c_2$ and $w_{ij} = w$ for all i and j. In all the simulation results presented in this Note, we use the same parameter values:

$$c_2 = 0.8, \quad w = 0.8$$

In fact, the performances of many simulation results could be improved if the parameters were finely turned. However, we deliberately use the same parameter values in different simulation examples to demonstrate the robustness of DCG. In addition, extensive simulation suggests that $w \in [0.5, 1]$ and $c_2 \in [0.7, 0.9]$ could lead to stable guidance performance in a wide range of guidance scenarios.

Unless otherwise stated, in all the simulation examples given in this Note, the acceleration magnitude is saturated by 50 m/s^2, a vehicle stops moving when its range to the target is less than 20 m, and the simulation step size is fixed as 0.1 s.

A. Two-Dimensional Guidance Scenarios

In this section, we verify the performance of the 2-D version of DCG in Eq. (9).

First of all, consider a scenario of three vehicles and one stationary target in the plane. The initial states are given in Table 1. The communication topology of the vehicles is shown in Fig. 10.

1) The simulation results by PNG are given in Fig. 4. As can be seen, the maximum difference of the arrival time of the three vehicles is about 30 s.

2) The simulation results by DCG are shown in Fig. 5. As can be seen, both target interception and arrival time synchronization are achieved. The acceleration command of each vehicle converges to zero eventually.

3) The simulation results by DCG in the presence of communication delays and measurement noises are given in Fig. 6. In this example, noises are added to the measurements of v_i, r_i, $\dot{r}_i$, and η_i. The signal-to-noise ratio (SNR) is set to be 50 dB. Moreover, information transfer in every communication link has a time delay of 0.5 s.

4) Because the second term in the proposed guidance law contains η_i, if η_i is zero, then vehicle i actually cuts off its coordination with the other vehicles. This extreme case is examined in a simulation example shown in Fig. 7, where $\eta_1(0) = \eta_2(0) = 0$. As can be seen, vehicles 1 and 2 do not coordinate with the others and they approach the target along straight lines. Vehicle 3 still attempts to synchronize its final arrival time with the others by taking its maximum maneuverability. One important implication of this example is that the guidance law does not collapse in the extreme case of $\eta_i(0) = 0$.

5) In our guidance law design, we omit the third term $r_i\ddot{\eta}_i/3$ in Eq. (5). To evaluate its impact, we show the simulation results by DCG plus this term in Fig. 8. Note that $\ddot{\eta}_i = \dot{a}_i/v_i - \ddot{\lambda}_i$ is difficult to compute in a numerical simulation. In our simulation, to avoid an algebraic loop in MATLAB, we have to use delayed acceleration signals and a derivative Simulink block to compute this term. Such a way would certainly introduce some numerical errors, but it at least could show us the impact of the third term. As shown in Fig. 8, the cooperative guidance is successfully achieved but the acceleration commands are chattering. Here, the simulation step size is 0.3 s and the acceleration commands are first filtered by a first-order transfer function $1/(s + 1)$, which approximates the actuator dynamics. One

Table 1 Initial states in the first 2-D guidance scenario

	Position, m	Speed, m/s	Heading angle, deg
Target	[0, −2000]	0	NA
Vehicle 1	[−5500, −2000]	210	135
Vehicle 2	[0, −7000]	220	45
Vehicle 3	[6000, −4000]	230	60

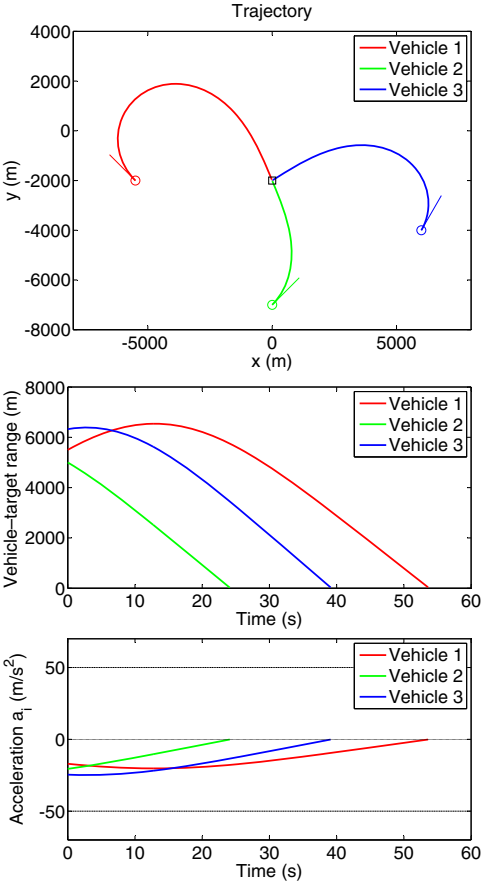

Fig. 4 Guidance results by PNG.

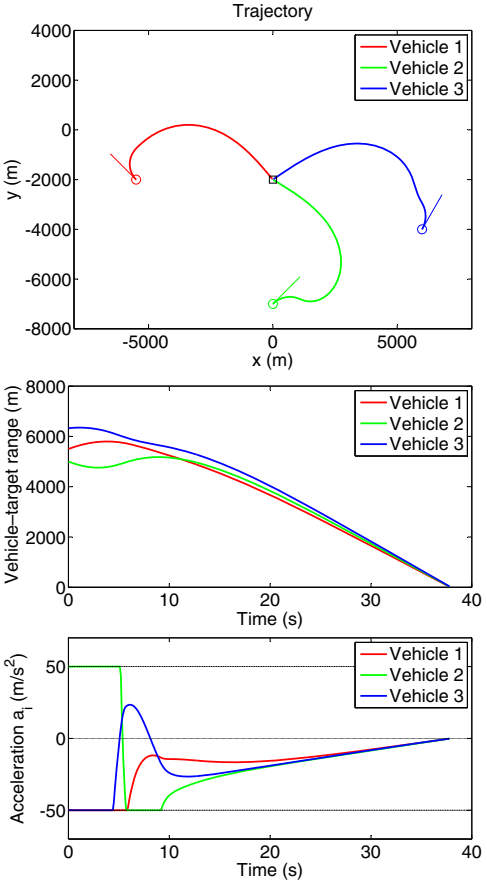

Fig. 5 Guidance results by DCG.

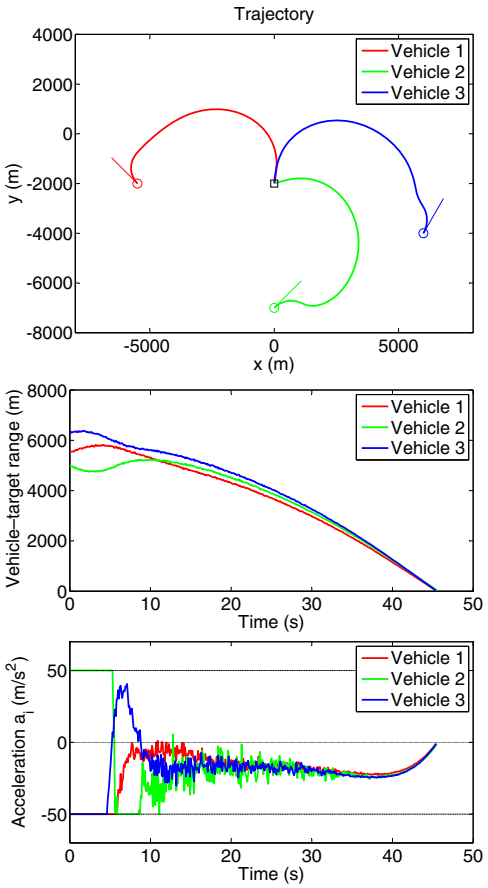

Fig. 6 Guidance results by DCG in the presence of communication delays (0.5 s) and measurement noise (50 dB SNR).

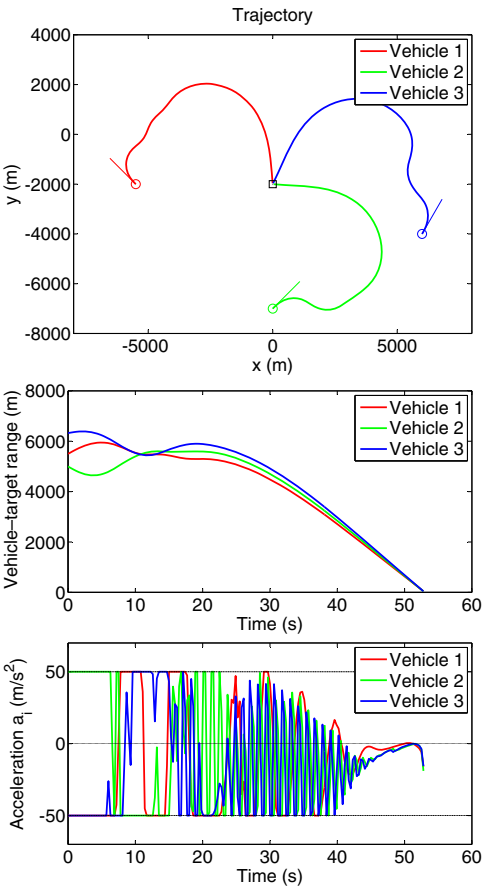

Fig. 8 Guidance results by DCG plus the term $r_i\ddot{\eta}_i/3$.

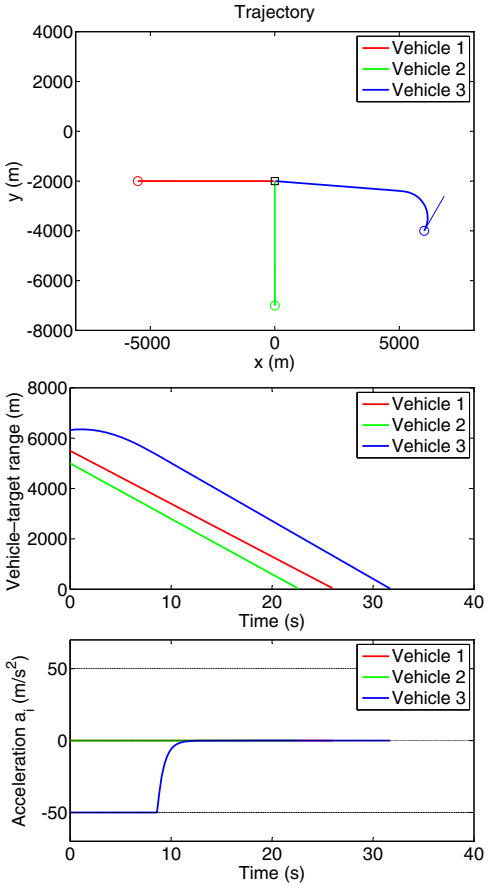

Fig. 7 Guidance results by DCG when $\eta_1(0) = \eta_2(0) = 0$.

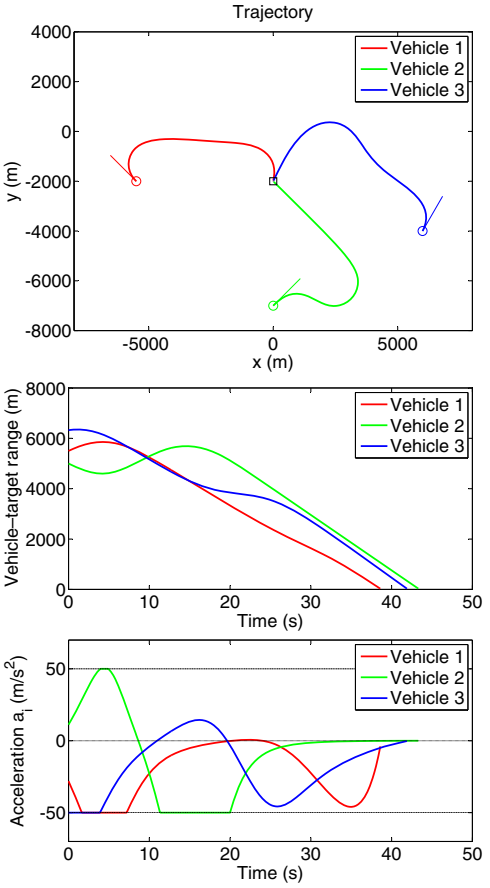

Fig. 9 Guidance results by CPN in Ref. [7].

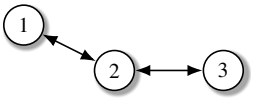

Fig. 10 Network topology of the 2-D simulation scenario.

important implication of this example is that omitting the third term does not yield noticeable performance decay, which justifies the design of our guidance law.

6) The guidance law proposed in Ref. [7], called cooperative proportional navigation (CPN), is regarded as a classic result in the literature. For the purpose of comparison, we use the same simulation scenario to examine the performance of CPN. Because CPN is designed for all-to-all graphs, we modify the underlying graph to be complete in this example. The other setup remains the same. When the graph is complete, the results of DCG remain similar and are omitted here due to space limitation.

CPN has a parameter K that must be selected appropriately. It was suggested in Ref. [7] (section IV) that K could be selected as $K^* = 40/(\bar{r}_0\bar{t}_{go0})$, where $\bar{r}_0$ and $\bar{t}_{go0}$ are the initial average values of the vehicle–target range and time to go. In this example, $K^* = 2.1 \times 10^{-4}$. However, we choose $K = K^*/3$ to obtain a better performance than $K = K^*$. As shown in Fig. 9, the performance of CPN is not as good as DCG in the sense that its trajectory is more curly and the final arrival time error is larger. Extensive simulation shows that the guidance performance of CPN is sensitive to the value of K.

Second of all, to further examine the robustness of DCG, we consider the following challenging scenarios.

1) Large initial velocity leading angles are challenging to handle for many guidance laws. Motivated by this, we examine DCG in an extreme case of $\eta_i = \pi$. The pure PNG law fails in this case, as shown in Figs. 11a and 11b. As a comparison, DCG still works effectively in this extreme case, as shown in Figs. 11c and 11d.

2) In the example, we consider a challenging case where the arrival time differences among the vehicles by pure PNG are extremely large. As shown in Figs. 12a and 12b, the maximum arrival time difference by PNG is more than 100 s. In this extreme case, DCG still works effectively and the final arrival time difference is reduced to about 1 s. In this example, acceleration saturation is still incorporated. The final arrival time error could be further reduced if w and c_2 are finely tuned.

In this example, due the large time difference, the vehicles take many detours to synchronize their arrival time. It must be noted that the main purpose of this example is to illustrate the strong robustness of DCG. In practice, too many trajectory detours may not be acceptable for certain vehicles such as missiles. One potential method to solve this problem is to choose small edge weights if two vehicles have an extremely large arrival time difference. In this way, we put target interception as priority and time synchronization as secondary to avoid unreasonable trajectory detours.

B. Three-Dimensional Guidance Scenarios

In this section, we verify the 3-D version of DCG in Eq. (15).

Consider a scenario where there are six vehicles and one stationary target. The initial parameters are given in Table 2. The communication topology of the six vehicles is shown in Fig. 13. Because the

Table 2 Initial states in the first 3-D guidance scenario

	Position, m	Initial velocity, m/s
Target	[0, −2000, 0]	[0, 0, 0]
Vehicle 1	[−5000, 2000, 3000]	[210, 0, 0]
Vehicle 2	[−5000, 4000, 4000]	[220, 0, 0]
Vehicle 3	[−5000, 6000, 3000]	[230, 0, 0]
Vehicle 4	[5000, 2500, 3000]	[−240, 0, 0]
Vehicle 5	[5000, 4500, 4000]	[−250, 0, 0]
Vehicle 6	[5000, 6500, 3000]	[−260, 0, 0]

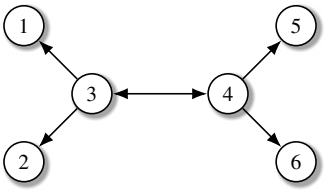

Fig. 13 Network topology of the 3-D simulation scenario. The graph is directed.

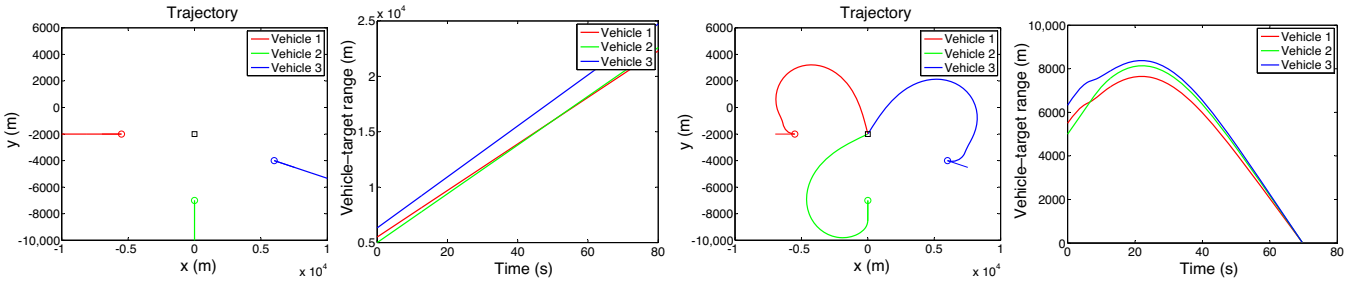

a) Trajectory by PNG **b) Vehicle–target range by PNG** **c) Trajectory by DCG** **d) Vehicle–target range by DCG**

Fig. 11 Challenging scenario with $\eta_i = \pi$ for all i. PNG fails but DCG works effectively.

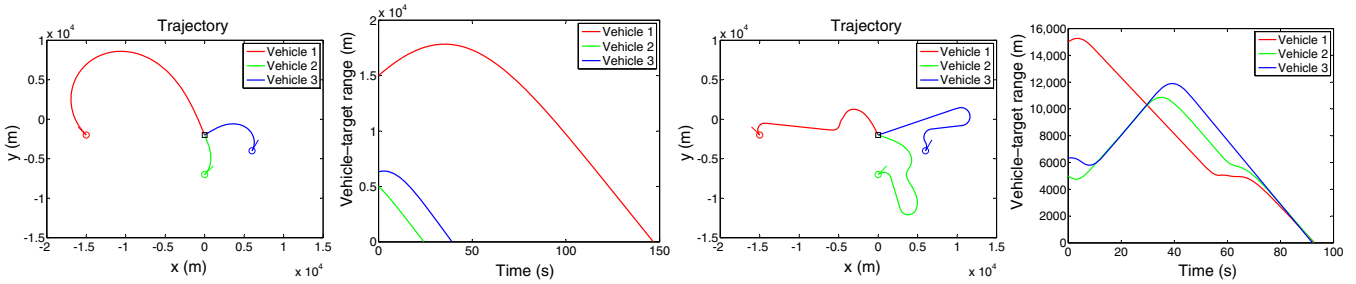

a) Trajectory by PNG **b) Vehicle–target range by PNG** **c) Trajectory by DCG** **d) Vehicle–target range by DCG**

Fig. 12 Challenging scenario where the arrival time difference is greater than 100 s by PNG. DCG still works effectively in this case.

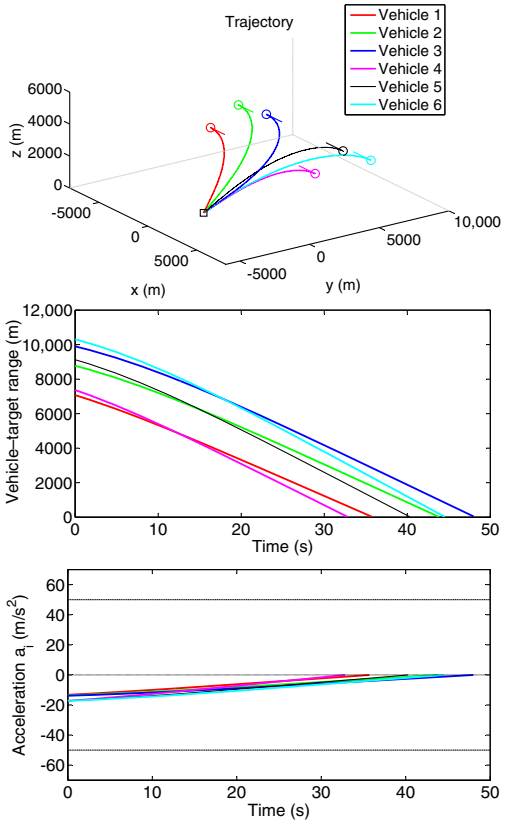

Fig. 14 3-D simulation results by PNG.

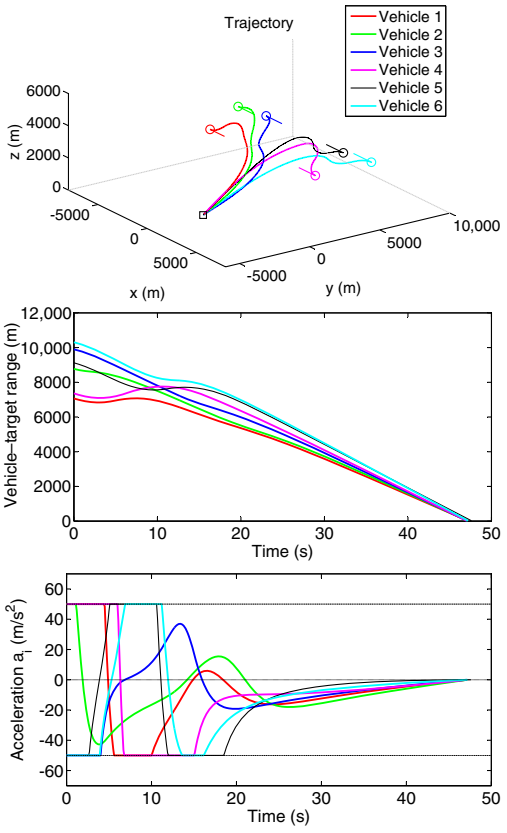

Fig. 15 3-D simulation results by DCG.

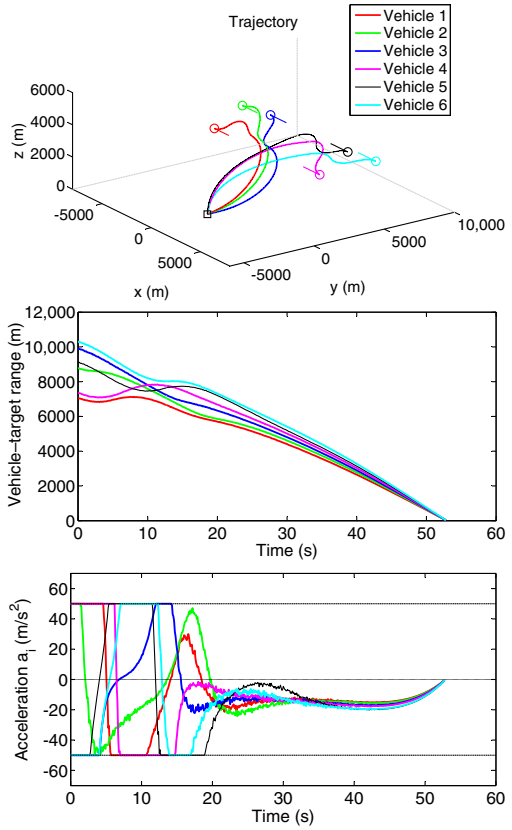

Fig. 16 3-D simulation results by DCG in the challenging scenario with measurement noises (60 dB SNR), and communication delays (0.5 s).

graph is directed, the final arrival time is jointly determined by vehicles 3 and 4.

The simulation results by PNG and DCG are shown in Figs. 14–16, respectively. As can be seen, DCG works effectively (see Fig. 15), even in the presence of measurement noise and communication delay (see Fig. 16).

VI. Conclusions

This Note proposed a new distributed cooperative guidance law for multivehicle simultaneous arrival. Compared to the existing guidance laws, the proposed one has the following merits. It has a concise biased-PNG expression and could be implemented in a distributed manner. It does not have any numerical singularities or require the estimation of time to go. Extensive simulation showed that the guidance law performs effectively in a wide range of scenarios, even in the presence of some challenging problems such as measurement noise, communication delay, large initial leading angles, and large initial arrival time difference.

The proposed guidance law could be generalized in several directions. First, fixed time or prescribed time could be incorporated into the guidance law if the arrival time is required to synchronize as soon as possible. Second, communication resources among vehicles are valuable in practice. Hence, it is meaningful to incorporate event-trigger techniques into cooperative guidance to reduce communication burden. Finally, the proposed guidance law is designed for stationary targets and constant velocity speed. How to handle maneuvering targets and time-varying vehicle speed is an important direction for future research.

Acknowledgments

This research work is supported by the National Natural Science Foundation of China (grant nos. 61903308, 61873031, and 61773031).

References

[1] Jeon, I. S., Lee, J. I., and Tahk, M. J., "Impact-Time-Control Guidance Law for Anti-Ship Missiles," *IEEE Transactions on Control Systems Technology*, Vol. 14, No. 2, 2006, pp. 260–266. https://doi.org/10.1109/TCST.2005.863655

[2] Zhao, S., Zhou, R., Wei, C., and Ding, Q., "Design of Time-Constrained Guidance Laws via Virtual Leader Approach," *Chinese Journal of Aeronautics*, Vol. 23, No. 1, 2010, pp. 103–108. https://doi.org/10.1016/S1000-9361(09)60193-X

[3] Kim, M., Jung, B., Han, B., Lee, S., and Kim, Y., "Lyapunov-Based Impact Time Control Guidance Laws Against Stationary Targets," *IEEE Transactions on Aerospace and Electronic Systems*, Vol. 51, No. 2, 2015, pp. 1111–1122. https://doi.org/10.1109/TAES.2014.130717

[4] Saleem, A., and Ratnoo, A., "Lyapunov-Based Guidance Law for Impact Time Control and Simultaneous Arrival," *Journal of Guidance, Control, and Dynamics*, Vol. 39, No. 1, 2016, pp. 164–173. https://doi.org/10.2514/1.G001349

[5] Tekin, R., Erer, K. S., and Holzapfel, F., "Polynomial Shaping of the Look Angle for Impact-Time Control," *Journal of Guidance, Control, and Dynamics*, Vol. 40, No. 10, 2017, pp. 2668–2673. https://doi.org/10.2514/1.G002751

[6] Zhao, S., and Zhou, R., "Cooperative Guidance for Multimissile Salvo Attack," *Chinese Journal of Aeronautics*, Vol. 21, No. 6, 2008, pp. 533–539. https://doi.org/10.1016/S1000-9361(08)60171-5

[7] Jeon, I. S., Lee, J. I., and Tahk, M. J., "Homing Guidance Law for Cooperative Attack of Multiple Missiles," *Journal of Guidance, Control, and Dynamics*, Vol. 33, No. 1, 2010, pp. 275–280. https://doi.org/10.2514/1.40136

[8] Meyer, Y., Isaiah, P., and Shima, T., "On Dubins Paths to Intercept a Moving Target," *Automatica*, Vol. 53, March 2015, pp. 256–263. https://doi.org/10.1016/j.automatica.2014.12.039

[9] He, S., Wang, W., Lin, D., and Lei, H., "Consensus-Based Two-Stage Salvo Attack Guidance," *IEEE Transactions on Aerospace and Electronic Systems*, Vol. 54, No. 3, 2017, pp. 1555–1566. https://doi.org/10.1109/TAES.7

[10] Dhananjay, N., and Ghose, D., "Accurate Time-to-Go Estimation for Proportional Navigation Guidance," *Journal of Guidance, Control, and Dynamics*, Vol. 37, No. 4, 2014, pp. 1378–1383. https://doi.org/10.2514/1.G000082

[11] Cho, N., and Kim, Y., "Modified Pure Proportional Navigation Guidance Law for Impact Time Control," *Journal of Guidance, Control, and Dynamics*, Vol. 39, No. 4, 2016, pp. 852–872. https://doi.org/10.2514/1.G001618

[12] Olfati-Saber, R., and Murray, R. M., "Consensus Problems in Networks of Agents with Switching Topology and Time-Delays," *IEEE Transactions on Automatic Control*, Vol. 49, No. 9, 2004, pp. 1520–1533. https://doi.org/10.1109/TAC.2004.834113

[13] Ren, W., and Beard, R. W., "Consensus Seeking in Multiagent Systems Under Dynamically Changing Interaction Topologies," *IEEE Transactions on Automatic Control*, Vol. 50, No. 5, 2005, pp. 655–661. https://doi.org/10.1109/TAC.2005.846556

[14] Lin, Z., Francis, B., and Maggiore, M., "Necessary and Sufficient Graphical Conditions for Formation Control," *IEEE Transactions on Automatic Control*, Vol. 50, No. 1, 2005, pp. 121–127. https://doi.org/10.1109/TAC.2004.841121

[15] Li, Z., Duan, Z., Chen, G., and Huang, L., "Consensus of Multiagent Systems and Synchronization of Complex Networks: A Unified Viewpoint," *IEEE Transactions on Circuits and Systems I: Regular Papers*, Vol. 57, No. 1, 2010, pp. 213–224. https://doi.org/10.1109/TCSI.2009.2023937

[16] Ren, W., and Beard, R. W., *Distributed Consensus in Multi-Vehicle Cooperative Control*, Springer, London, 2008, Chap. 4.

[17] Zhao, Q., Dong, X., Liang, Z., Bai, C., Chen, J., and Ren, Z., "Distributed Cooperative Guidance for Multiple Missiles with Fixed and Switching Communication Topologies," *Chinese Journal of Aeronautics*, Vol. 30, No. 4, 2017, pp. 1570–1581. https://doi.org/10.1016/j.cja.2017.06.009

[18] Kang, S., Wang, J., Li, G., Shan, J., and Petersen, I. R., "Optimal Cooperative Guidance Law for Salvo Attack: An MPC-Based Consensus Perspective," *IEEE Transactions on Aerospace and Electronic Systems*, Vol. 54, No. 5, 2018, pp. 2397–2410. https://doi.org/10.1109/TAES.2018.2816880

[19] Song, L., Zhang, Y., Huang, D., and Fu, S., "Cooperative Simultaneous Attack of Multi-Missiles Under Unreliable and Noisy Communication Network: A Consensus Scheme of Impact Time," *Aerospace Science and Technology*, Vol. 47, Dec. 2015, pp. 31–41. https://doi.org/10.1016/j.ast.2015.09.015

[20] Kim, B. S., Lee, J. G., and Han, H. S., "Biased PNG Law for Impact with Angular Constraint," *IEEE Transactions on Aerospace and Electronic Systems*, Vol. 34, No. 1, 1998, pp. 277–288. https://doi.org/10.1109/7.640285

[21] Zhang, Y., Wang, X., and Wu, H., "A Distributed Cooperative Guidance Law for Salvo Attack of Multiple Anti-Ship Missiles," *Chinese Journal of Aeronautics*, Vol. 28, No. 5, 2015, pp. 1438–1450. https://doi.org/10.1016/j.cja.2015.08.009

[22] He, S., and Lee, C. H., "Optimal Proportional-Integral Guidance with Reduced Sensitivity to Target Maneuvers," *IEEE Transactions on Aerospace and Electronic Systems*, Vol. 54, No. 5, 2018, pp. 2568–2579. https://doi.org/10.1109/TAES.2018.2824678

[23] Yu, W., Chen, G., and Cao, M., "Some Necessary and Sufficient Conditions for Second-Order Consensus in Multi-Agent Dynamical Systems," *Automatica*, Vol. 46, No. 6, 2010, pp. 1089–1095. https://doi.org/10.1016/j.automatica.2010.03.006

[24] Meng, Z., Ren, W., Cao, Y., and You, Z., "Leaderless and Leader-Following Consensus with Communication and Input Delays Under a Directed Network Topology," *IEEE Transactions on Systems, Man, and Cybernetics, Part B (Cybernetics)*, Vol. 41, No. 1, 2010, pp. 75–88. https://doi.org/10.1109/TSMCB.2010.2045891

[25] Lin, P., and Jia, Y., "Consensus of a Class of Second-Order Multi-Agent Systems with Time-Delay and Jointly-Connected Topologies," *IEEE Transactions on Automatic Control*, Vol. 55, No. 3, 2010, pp. 778–784. https://doi.org/10.1109/TAC.2010.2040500

[26] Chen, Y., Wang, J., Wang, C., Shan, J., and Xin, M., "A Modified Cooperative Proportional Navigation Guidance Law," *Journal of the Franklin Institute*, Vol. 356, No. 11, 2019, pp. 5692–5705. https://doi.org/10.1016/j.jfranklin.2019.04.013

[27] Song, S. H., and Ha, I. J., "A Lyapunov-Like Approach to Performance Analysis of 3-Dimensional Pure PNG Laws," *IEEE Transactions on Aerospace and Electronic Systems*, Vol. 30, No. 1, 1994, pp. 238–248. https://doi.org/10.1109/7.250424

[28] Zhao, J., Zhou, R., and Dong, Z., "Three-Dimensional Cooperative Guidance Laws Against Stationary and Maneuvering Targets," *Chinese Journal of Aeronautics*, Vol. 28, No. 4, 2015, pp. 1104–1120. https://doi.org/10.1016/j.cja.2015.06.003